

Niche theory for mutualism: A graphical approach to plant-pollinator network dynamics

Fernanda S. Valdovinos^{1,*}

Robert Marsland III²

September 3, 2020

1. University of California - Davis, Davis, CA 95616;

2. Boston University, Boston, Massachusetts 02215;

* Corresponding author; e-mail: fvaldovinos@ucdavis.edu.

The authors wish to be identified by the reviewers.

Keywords: Contemporary Niche Theory, Ecological Networks, Mutualistic Interactions, Pollination Ecology, Competition for pollination, Competition for floral rewards.

Number of words in the main text (excluding abstract, figure legends, tables, and literature cited):
5,810.

Manuscript elements: Figure 1, figure 2, figure 3, figure 4, table 1, table 2, online appendices A, B, C and D including figures S1, S2, S3 and S4.

Manuscript type: Article.

Code producing figures available at: github.com/robertvsiii/niche-mutualism

Prepared using the suggested L^AT_EX template for *Am. Nat.*

Abstract

Contemporary Niche Theory is a useful framework for understanding how organisms interact with each other and with their shared environment. Its graphical representation, popularized by Tilman's Resource Ratio Hypothesis, facilitates the analysis of the equilibrium structure of complex dynamical models including species coexistence. This theory has been applied primarily to resource competition since its early beginnings. Here, we integrate mutualism into niche theory by expanding Tilman's graphical representation to the analysis of consumer-resource dynamics of plant-pollinator networks. We graphically explain the qualitative phenomena previously found by numerical simulations, including the effects on community dynamics of nestedness, adaptive foraging, and pollinator invasions. Our graphical approach promotes the unification of niche and network theories, and deepens the synthesis of different types of interactions within a consumer-resource framework.

Secondary Abstract

Teoría de Nicho para Mutualismos: Una aproximación gráfica a la dinámica de redes planta-polinizador

La Teoría Contemporánea de Nicho es un marco útil para entender cómo los organismos interactúan entre ellos y con su ambiente compartido. Su representación gráfica, popularizada por la Hipótesis de Razón de Recursos de Tilman, facilita el análisis de la estructura de equilibrio de modelos dinámicos complejos, incluyendo la coexistencia de especies. Esta teoría ha sido aplicada primariamente a competencia por recursos desde sus inicios. Aquí, integramos el mutualismo dentro de la teoría de nicho al expandir la representación gráfica de Tilman al análisis de la dinámica consumidor-recurso de las redes planta-polinizador. Explicamos gráficamente fenómenos cualitativos encontrados previamente mediante simulaciones numéricas, incluyendo los efectos sobre la dinámica comunitaria del anidamiento, forrajeo adaptativo y de las invasiones por polinizadores. Nuestra aproximación gráfica promueve la unificación de las teorías de nicho

y de redes, y profundiza la síntesis de diferentes tipos de interacciones dentro de un marco de consumidor-recurso.

Introduction

2 Mutualistic interactions pervade every type of ecosystem and level of organization on Earth
(Boucher et al. 1982; Bronstein 2015). Mutualisms such as pollination (Ollerton et al. 2011), seed
4 dispersal (Wang and Smith 2002), coral symbioses (Rowan 2004), and nitrogen-fixing associations
between plants and legumes, bacteria, or fungi (Horton and Bruns 2001; van der Heijden et al.
6 2008) sustain the productivity and biodiversity of most ecosystems on the planet and human
food security (Potts et al. 2016; Ollerton 2017). However, ecological theory on mutualisms has
8 been scarce and less integrated than for predation and competition, which hinders our ability
to protect, manage, and restore mutualistic systems (Vandermeer and Boucher 1978; Bascompte
10 and Jordano 2014; Bronstein 2015). This scarce theoretical development is of particular concern
because several mutualisms such as coral-algae and plant-pollinator that play a critical role in the
12 functioning of ecosystems are currently under threat (Brown 1997; Rowan 2004; Goulson et al.
2015; Ollerton 2017). In particular, Niche Theory (MacArthur 1969, 1970; Tilman 1982; Leibold
14 1995; Chase and Leibold 2003) for mutualisms has only recently started to be developed (Peay
2016; Johnson and Bronstein 2019). Chase and Leibold (2003) suggest that Contemporary Niche
16 Theory can be expanded to mutualism, but such suggestion has yet to be explored. Here, we ex-
pand niche theory to mutualistic networks of plant-pollinator interactions by further developing
18 the graphical approach popularized by Tilman (1982) to analyze a consumer-resource dynamic
model of plant-pollinator networks developed, analyzed, and tested by Valdovinos et al. (2013,
20 2016, 2018).

For about 70 years, theoretical research analyzing the population dynamics of mutualisms
22 roughly only assumed Lotka-Volterra type models (*sensu* Valdovinos 2019) to conduct their stud-
ies (e.g., Kostitzin 1934; Gause and Witt 1935; Vandermeer and Boucher 1978; Wolin and Lawlor
24 1984; Bascompte et al. 2006; Okuyama and Holland 2008; Bastolla et al. 2009). Those models
represent mutualistic relationships as direct positive effects between species using a (linear or
26 saturating) positive term in the growth equation of each mutualist that depends on the popula-

tion size of its mutualistic partner. While this research increased our understanding of the effects
28 of facultative, obligate, linear, and saturating mutualisms on the long-term stability of mutualistic
systems, more sophisticated understanding of their dynamics (e.g., transients) and of phenom-
30 ena beyond the simplistic assumptions of the Lotka-Volterra type models was extremely scarce.
A more mechanistic consumer-resource approach to mutualisms has been recently proposed by
32 Holland and colleagues (Holland et al. 2005; Holland and DeAngelis 2010) and further devel-
oped by Valdovinos et al. (2013, 2016, 2018). This approach decomposes the net effects assumed
34 always positive by Lotka-Volterra type models into the biological mechanisms producing those
effects including the gathering of resources and exchange of services.

36 The key advance of the consumer-resource model developed by Valdovinos et al. (2013) is
separating the dynamics of the plants' vegetative biomass from the dynamics of the plants' floral
38 rewards. This separation allows: i) tracking the depletion of floral rewards by pollinator con-
sumption, ii) evaluating exploitative competition among pollinator species consuming the floral
40 rewards provided by the same plant species, and iii) incorporating the capability of pollinators
(adaptive foraging) to behaviorally increase their foraging effort on the plant species in their diet
42 with more floral rewards available. Another advance of this model is incorporating the dilu-
tion of conspecific pollen carried by pollinators, which allows tracking competition among plant
44 species for the quality of pollinator visits (see next section).

46 This contribution analyzes the dynamics of plant-pollinator networks when all the above-
mentioned biological mechanisms are considered. Specifically, we provide analytical understand-
48 ing for the results found with extensive numerical simulations (Valdovinos et al. 2013, 2016, 2018,
hereafter "previous simulations"), and generalize some of them beyond the original simulation
50 conditions. By "analytical understanding" we refer to finding those results using a graphical ap-
proach whose geometry rigorously reflects mathematical analysis (Tilman 1982; Koffel et al. 2016,
also provided in our Appendices). Our Methods describe the Valdovinos et al.'s model and our
52 graphical approach, including the conditions for coexistence among adaptive pollinators sharing
floral rewards and how we use projections to analyze high-dimensional systems. Our Results

54 first demonstrate the effects of nestedness on species coexistence in networks without adaptive
foraging found by previous simulations (Valdovinos et al. 2016). Nestedness is the tendency
56 of generalists (species with many interactions) to interact with both generalists and specialists
(species with one or a few interactions), and of specialists to interact with only generalists. Sec-
58 ond, we demonstrate the effects of adaptive foraging on species coexistence in nested networks
found by the same simulation study. Third, we demonstrate the impacts of pollinator invasions
60 on native pollinators in nested networks with adaptive foraging found numerically by Valdovi-
nos et al. (2018). Finally, we discuss how our approach helps to integrate niche and network
62 theories, and deepens the synthesis of different types of interactions within a consumer-resource
framework.

64

Methods

1. *Dynamical model of plant-pollinator interactions*

66 Valdovinos et al. (2013) model the population dynamics of each plant and pollinator species
of the network, as well as the dynamics of floral rewards and pollinators' foraging preferences
68 (see Table 1 for definitions of variables and parameters). Four functions define these dynamics.
The function $V_{ij}(p_i, a_j) = \alpha_{ij}\tau_{ij}a_jp_i$ represents the visitation rate of animal species j to plant
70 species i and connects the dynamics of plants, animals, rewards, and foraging preferences. An
increase in visits increases plant growth rate via pollination and animal growth rate via rewards
72 consumption, but decreases rewards availability. The function $\sigma_{ij}(p_k) = \frac{\alpha_{ij}\tau_{ij}p_i}{\sum_{k \in P_j} \alpha_{kj}\tau_{kj}p_k}$ represents
the fraction of j 's visits that successfully pollinate plant i , and accounts for the dilution of plant
74 i 's pollen when j visits other plant species. Pollinators visiting many different plant species carry
more diluted pollen (low quality visits) than the pollen carried by pollinators visiting only one
76 plant species (high quality visits). The function $\gamma_i(p_k) = g_i(1 - \sum_{l \neq i \in P} u_l p_l - w_i p_i)$ represents
the germination rate of the seeds produced by the successful pollination events, where g_i is
78 the maximum fraction of i -recruits subjected to both inter-specific (u_l) and intra-specific (w_i)

competition. Finally, the function $f_{ij}(R_i/p_i) = b_{ij} \frac{R_i}{p_i}$ represents the rewards consumption by animal j in each of its visits to plant i . These functions capturing the above mentioned biological processes lead to the following equations:

$$\frac{dp_i}{dt} = \underbrace{\gamma_i(p_k)}_{\text{germination rate}} \sum_{j \in A_i} \underbrace{e_{ij}\sigma_{ij}(p_k)V_{ij}(p_i, a_j)}_{\text{seed production}} - \underbrace{\mu_i^P p_i}_{\text{mortality}} \quad (1)$$

$$\frac{da_j}{dt} = \sum_{i \in P_j} \underbrace{c_{ij}V_{ij}(p_i, a_j)f_{ij}(R_i/p_i)}_{\text{rewards consumption}} - \underbrace{\mu_j^A a_j}_{\text{mortality}} \quad (2)$$

$$\frac{dR_i}{dt} = p_i \underbrace{\left[\beta_i - \phi_i \frac{R_i}{p_i} \right]}_{\text{per-plant rewards production}} - \sum_{j \in A_i} \underbrace{V_{ij}(p_i, a_j)f_{ij}(R_i/p_i)}_{\text{rewards consumption}} \quad (3)$$

$$\frac{d\alpha_{ij}}{dt} = \frac{G_j \alpha_{ij}}{a_j} \left(c_{ij} \underbrace{V_{ij}^s(p_i, a_j)f_{ij}(R_i/p_i)}_{\text{rewards consumption as specialist}} - \sum_{k \in P_j} c_{kj} \underbrace{V_{kj}(p_k, a_j)f_{kj}(R_k/p_k)}_{\text{actual rewards consumption}} \right), \quad (4)$$

where $V_{ij}^s = \tau_{ij}a_jp_i$ is the visitation rate of animal species j to plant species i under a pure specialist strategy $\alpha_{ij} = 1$. That is, the preference of animal j for plant i increases when the rewards that could be extracted from plant species i by application of full foraging effort to that plant ($\alpha_{ij} = 1$) exceed the rewards currently obtained from all plants in j 's diet. The preference decreases in the opposite case, where the rewards obtainable by exclusive foraging on plant i are lower than the current rewards uptake level. Note that the terms in Eq. (4) have been re-arranged from previous publications of this model to emphasize the coupling of the four equations through the visitation rates V_{ij} . We use parentheses that include the variables determining each of the functions in the equations to distinguish functions from parameters, but in the text those parentheses are excluded for better readability. The visitation rate V_{ij} and the rewards extracted per visit f_{ij} can also be modeled by a saturating function following Holling's Type II functional response (Holling 1959), as discussed in Appendix D.

The sums in equations (1-4) are taken over the sets of A_i and P_j of pollinator species that are capable of visiting plant i , and plant species that can be visited by pollinator j , respectively. Those sets are defined by the network structure taken as model input. Finally, the dynamic preferences

Symbol	Meaning
p_i	plant abundance per unit area ([ind.]/m ²)
a_j	animal (pollinator) abundance per unit area ([ind.]/m ²)
R_i	reward abundance per unit area (g/m ²)
α_{ij}	foraging preference (dimensionless)
g_i	max germination rate ([ind.]/[seeds])
u_l	plant inter-specific competition (m ² /[ind.])
w_i	plant intra-specific competition (m ² /[ind.])
e_{ij}	expected number of seeds per pollination event ([seeds]/[visits])
τ_{ij}	visitation efficiency ([visits]m ² /[ind.] ² yr)
$\mu_i^{P/A}$	mortality rates (1/yr)
c_{ij}	conversion efficiency of rewards into animal abundance ([ind.]/g)
b_{ij}	per-visit rewards extraction (1/[visits])
β_i	per-plant reward production (g/[ind.]yr)
ϕ_i	self-limitation of reward production (1/yr)
G_j	adaptation rate (dimensionless)

Table 1: Model variables and parameters

of Eq. (4) model adaptive foraging. These preferences are restricted by $\sum_{k \in P_j} \alpha_{kj} = 1$. When
98 adaptive foraging is not considered, foraging preferences are fixed to:

$$\alpha_{ij} = \frac{1}{P_j} \quad (5)$$

where P_j here represents the number of plant species visited by pollinator species j .

100 *2. Niche theory for plant-pollinator dynamics*

“Niche” is a central concept in ecology, significantly clarified and refined over the past fifty years
102 (MacArthur 1969, 1970; Tilman 1982; Leibold 1995; Chase and Leibold 2003). We analyze the
niche of plant and pollinator species within their mutualistic interactions, assuming all their
104 other niche variables (e.g., soil nutrients, water, temperature, nesting sites) constant and suffi-
cient for supporting their populations. There are two reasonable choices for the definition of
106 environment space in plant-pollinator systems. First, on short timescales (i.e., within a flowering
season, “Rewards Space”, Fig. 1a), the plant populations can be regarded as constant and the
108 relevant environmental factors are the floral rewards. Second, on longer timescales (i.e., across
several flowering seasons, “Plant Space”, Fig. 1b), plant populations represent the axes for the
110 environment space, letting the reward levels implicitly determine the value of each plant popula-
tion as a food source. Table 2 summarizes both representations in terms of the model parameters.
112 This section explains both representations to provide a broader picture of niche theory applied
to plant-pollinator systems, but we obtain our results on Rewards Space.

114 The “requirement niche” of each pollinator species j ($j = 1, 2, \dots, A$) in either Rewards or
Plant Space can be encoded by a zero-net-growth isocline (ZNGI) (Tilman 1982; Leibold 1995).
116 The ZNGI is a hypersurface that separates the environmental states where the growth rate is
positive from the states where it is negative. Environmental states along the ZNGI support animal
118 reproduction rates that exactly balance mortality rates, leading to constant population sizes.
Adaptive foraging allows the ZNGIs in Rewards Space to dynamically rotate in the direction

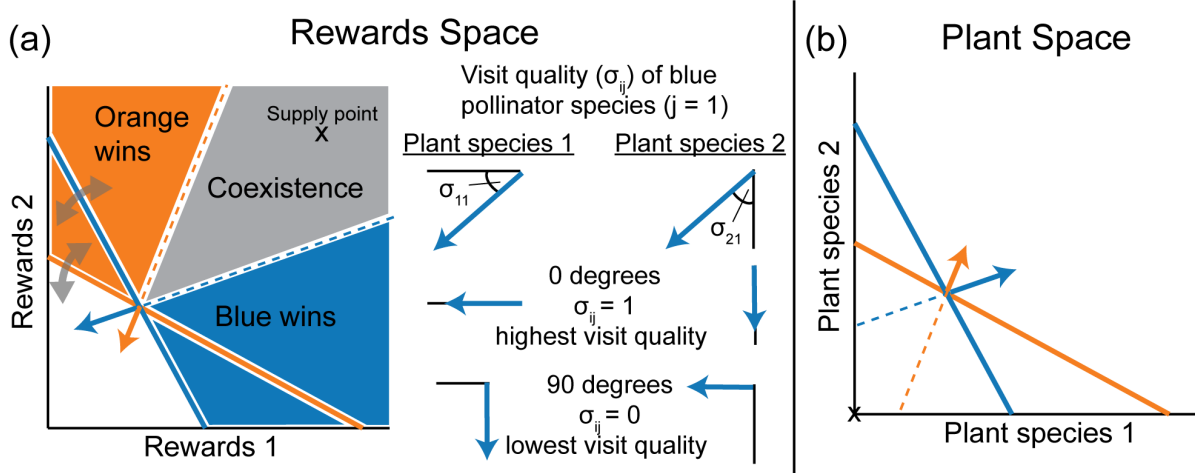


Figure 1: **Niche theory for mutualism.** (a) Representation of plant-pollinator system as a standard consumer-resource type model, for timescales on which plant populations are approximately constant. Impact vectors and ZNGIs are shown for two pollinator species (blue and orange) competing for the rewards of two plant species. Adaptive foraging causes the ZNGIs and impact vectors to rotate in the direction of the most abundant resource, as discussed in detail in Appendix A. The angle between the impact vector and a given rewards axis affects the pollinator's visit quality for the corresponding plant, with zero degrees corresponding to $\sigma_{ij} = 1$ (highest visit quality), and 90 degrees corresponding to $\sigma_{ij} = 0$ (lowest visit quality). See supplementary figure S2 for detailed discussion of angle-quality relationship. (b) Representation in terms of plant populations for analysis of longer timescales, where the mutualism becomes visible. The "supply point" is now located at the origin, and the pollinator impacts are necessary to sustain nonzero plant abundance. The location of the ZNGIs depends on the current nutritional value of each plant species, which is lower for species whose floral rewards are more depleted. The impact vectors (see Table 2) depend on both the visit quality and the per-capita visit frequency of each pollinator species (σ_{ij} and V_{ij}/a_j of Eq. (1), respectively), and encode each pollinator's contribution to the total number of seedlings in the next generation.

120 of the most abundant rewards. The ZNGIs are dynamic in Plant Space (even in the absence of
121 adaptive foraging) because the contribution each plant makes to the animal growth rate depends
122 on the current reward level.

123 The “impact niche” of each pollinator species is represented by an *impact vector*, which speci-
124 fies the magnitude and direction of the environmental change induced by an average individual
125 of the species (Tilman 1982; Leibold 1995). In Rewards Space, the impact of a pollinator species
126 is the rate at which it depletes the floral rewards, just as in traditional models of resource com-
127 petition, but its angle takes on a new importance in connection with the visit quality σ_{ij} . A
128 nearly perpendicular impact vector to a given rewards axis means that only a small fraction of
129 the pollinator’s visits are allocated to the corresponding plant, and most of the pollen carried
130 by this pollinator belongs to other plant species. A plant species will eventually go extinct if all
131 its visits have such low quality (see below). Note that the exact mapping from the angle to the
132 visit quality depends on the foraging strategy, number of plant species, and plant abundances
133 (see Fig. S2 of Appendix C). In Plant Space, the positive effects of plant-pollinator mutualisms
134 are directly visible in the impact vectors pointing to larger plant population sizes (as opposed
135 to pointing to smaller population sizes in the traditional models of resource competition), and
136 represent the number of successful pollination events caused by each pollinator species.

137 The environment also has its intrinsic dynamics, represented by a *supply vector* (Tilman 1982;
138 Chase and Leibold 2003). In Rewards Space, the supply vector points towards the *supply point*
139 where the rewards reach equilibrium in the absence of pollinators (like in traditional models of
140 resource competition). However, the supply point itself is determined by the plant populations,
141 which depend on pollination activity for their long-term survival. Extinction of a plant species
142 (e.g., due to low visit quality) causes the supply point to drop to zero along the corresponding
143 rewards axis, leading to a cascade of ecological reorganization and a new equilibrium (see below).
144 In Plant Space, the equilibrium point in the absence of pollinators is always at the origin, since
145 all plants require pollination services to avoid extinction.

146 These three quantities (ZNGIs, impact vectors, and supply point) define the conditions for

Rewards Space		
Niche concept	Description	Mathematical expression
ZNGI	Reproduction/mortality balance	$\sum_{i \in P_j} c_{ij} (V_{ij} / a_j) f_{ij} = \mu_j^A$
Impact Vector	Per-capita rewards consumption	$-(V_{ij} / a_j) f_{ij}$
Supply Point	Rewards equilibrium without animals	$\beta_i p_i / \phi_i$
Plant Space		
Niche concept	Description	Mathematical expression
ZNGI	Reproduction/mortality balance	$\sum_{i \in P_j} c_{ij} (V_{ij} / a_j) f_{ij} = \mu_j^A$
Impact Vector	Plant production	$\gamma_i e_{ij} \sigma_{ij} (V_{ij} / a_j)$
“Supply Point”	Plant equilibrium without animals	0

Table 2: Mapping elements of the model to niche theory concepts.

stable coexistence. Pollinator populations reach equilibrium when all the corresponding ZNGIs
¹⁴⁸ pass through the current environmental state. In addition, the combined impact of all pollinator species must exactly cancel the supply for the environment to remain in this state. This total
¹⁵⁰ impact is found by multiplying each impact vector by the corresponding population density, and then summing the results. Whenever the supply point lies within the cone formed by extending
¹⁵² all the impact vectors backwards (Fig. 1), a set of population densities can be found with a total impact equal and opposite to the supply. Each potentially stable set of coexisting species is thus
¹⁵⁴ represented by an intersection of ZNGIs, and coexistence is achieved whenever the supply point falls within the corresponding coexistence cone.

¹⁵⁶ *3. Conditions for adaptive pollinator coexistence on shared rewards*

The full equilibrium of the model also requires that adaptive foraging dynamics have reached a
¹⁵⁸ steady state. This requirement is satisfied with additional restrictions on the parameter values, which we derive by setting the pollinator growth rate $da_j/dt = 0$ in Eq. (2) and substituting into
¹⁶⁰ the adaptive foraging equation (4). We find the following equilibrium condition:

$$0 = \frac{G_j \alpha_{ij}}{a_j} (c_{ij} V_{ij}^s f_{ij} - \mu_j^A). \quad (6)$$

The term in parentheses is what the growth rate da_j/dt for animal species j would be if it
 162 were a specialist on plant species i , with $V_{ij} = V_{ij}^s$ and $\alpha_{ij} = 1$. Eq. (6) requires that this term
 vanish at equilibrium for all plant-animal pairs i, j where $\alpha_{ij} \neq 0$. Substituting in the expressions
 164 for V_{ij} and f_{ij} from the first section of the Methods, we find the equilibrium rewards abundance
 R_i^* :

$$R_i^* = \frac{\mu_j^A}{c_{ij} \tau_{ij} b_{ij}}. \quad (7)$$

166 This result imposes a strict constraint on the animal mortality rates μ_j^A and the reward uptake
 efficiencies $c_{ij} \tau_{ij} b_{ij}$, requiring that both terms vary in the same way from species to species, for
 168 all animals that share rewards from the same plant species i (i.e., for all animals with $\alpha_{ij} \neq$
 0). Pacciani-Mori et al. (2020) suggests that this required correlation between mortality rates
 170 and ingestion rates is consistent with allometric scaling relationships (Yodzis and Innes 1992).
 However, it is still unknown whether this relationship holds at the species level. Hereafter, we
 172 assume that the pollinators' ZNGIs intersect, acknowledging that the mechanism for coexistence
 is not present in our model.

174 Appendix A shows that R_i^* is the rotation center for the ZNGIs and, therefore, the shared R_i^*
 remains the point of intersection for all the ZNGIs over the entire course of adaptive foraging
 176 dynamics.

4. Using projections to analyze high-dimensional ecosystems

178 The graphical analysis described above is easily visualized for environmental spaces with two di-
 mensions. Plant-pollinator networks, however, contain tens to hundreds of plant species. In this
 180 full space, the ZNGIs are no longer lines but hypersurfaces of dimension $P - 1$ (Fig. 2b, where

P is the number of plant species in the network). The intersections among these hypersurfaces
182 determine the points of potential coexistence. We extend our graphical approach to many dimensions
184 and analyze the conditions for coexistence among the species whose ZNGI hypersurfaces
intersect by using projections of the coexistence cone onto two-dimensional slices through the
full environmental space.

186 We consider the two-dimensional slice where two of the rewards (or plant) abundances are
allowed to vary (gray plane in Fig. 2b), while all other abundances are held fixed at the values
188 where the intersection occurs. We then create a diagram like those of Fig. 1 by drawing the lines
where the ZNGIs intersect this slice, and projecting the impact vectors and supply point onto
190 this slice (i.e., taking the component parallel to the slice's surface). The species do not coexist if
the projection of the supply point lies outside the projection of the coexistence cone (e.g., Fig. 2a-
192 c), because this can only happen when the supply point lies outside the full coexistence cone.
But the supply point may still lie outside the cone (along one of the directions that has been
194 projected out) even if the projected supply point lies inside the projected coexistence cone. To
guarantee coexistence, one must examine all possible two-dimensional projections and ensure
196 that the supply point is inside the cone in every projection (Fig. S3).

Results

Effects of nestedness on network dynamics without adaptive foraging

198 Most plant-pollinator networks exhibit a nested structure (definition and citations provided in
200 the Introduction). The implications of nestedness for the stability of these networks have been
a topic of study for over a decade (Bastolla et al. 2009; Allesina and Tang 2012, reviewed in
202 Valdovinos 2019). Valdovinos et al. (2016) provide a more mechanistic framework to evaluate
the effects of nestedness on the dynamics of plant-pollinator networks. This section analytically
204 confirms their numerical results when pollinators are fixed foragers (Eq. 5), and provides criteria
for plant survival not found by previous work (see next section for adaptive foragers).

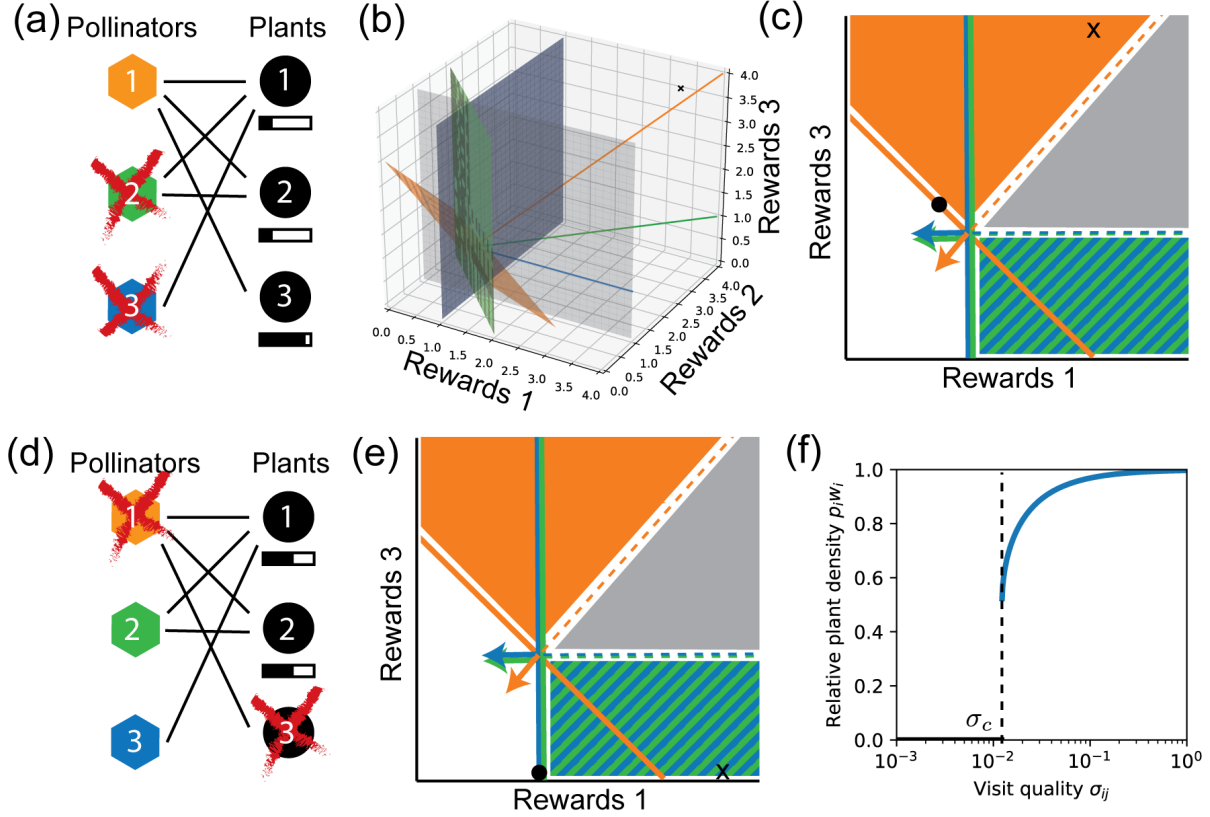


Figure 2: Effects of nestedness without adaptive foraging. (a) Nested network with three pollinator (polygons) and two plant (circles) species. Shaded bars indicate rewards abundance at the equilibrium point in panels *c* and *e*, with differences among species exaggerated for clarity. Red 'x' indicates extinction at equilibrium. (b) Three-dimensional ZNGIs, impact vectors, and supply point of this network. (c) ZNGIs and impact vectors projected onto the the rewards 1-rewards 3 plane (gray transparent plane in *b*). Pollinator species 2 and 3 have same projections onto this plane because both visit plant species 1 and none visit plant species 3 (see other projections in Fig. S3). Black dot indicates rewards at equilibrium. Specialist pollinators 2 and 3 go extinct because supply point (black 'x') falls in the orange zone. (d) Specialist plant species 3 goes extinct when the quality of visits it receives is lower than the threshold σ_c of panel *c*. (e) Supply point drops to zero along the rewards 3 axis when plant species 3 goes extinct, which results in the extinction of the generalist pollinator species 1. (f) Dependence of specialist plant abundance p_i on visit quality σ_{ij} , using Eq. (C5) from Appendix C. Minimal visit quality σ_c required for plant persistence is indicated by the dotted line. Parameters values are taken from Valdovinos et al. (2013), with: $\tau_{ij} = 1$, $e_{ij} = 0.8$, $\mu_i^P = 0.008$, $c_{ij} = 0.2$, $\mu_j^A = 0.004$, $b_{ij} = 0.4$, $g_i = 0.4$, $w_i = 1.2$, $\beta_i = 0.2$, $\phi_{ij} = 0.04$. Plant abundance is measured in units of the plant's carrying capacity $1/w_i$, so that the maximum possible value equals 1.

206 We perform our graphical analysis using two-dimensional slices through the full rewards
space of a nested 3-plant-3-pollinator-species network (Fig. 2a), which has sufficient complexity
208 to illustrate all the relevant projections for arbitrarily large networks. Fig. 2b shows the three-
dimensional rewards space, with the three colored planes being the ZNGIs of the three pollinator
210 species (derived from Table 2). The coexistence cone is the three-sided solid bounded by planes
connecting the backwards extensions of the impact vectors (colored lines). We project this cone
212 onto the gray transparent plane composed by rewards 1 and 3. This projection is depicted in
Fig. 2c, which shows the asymmetric shape of the coexistence cone, bounded on one side by the
214 impact vectors of the specialist pollinators (green and blue vectors parallel to rewards axis 1), and
on the other by the impact vector of the generalist pollinator species (diagonal orange vector).
216 This asymmetric shape is characteristic of nested networks since nestedness increases the diet
overlap between specialist and generalist species. This is one of only three possible cone shapes
218 in a two-dimensional projection (see Supplementary Fig. S4) regardless of the full environment
dimension

220 Valdovinos et al. (2016) show that increasing nestedness increases the extinction of specialist
species in networks without adaptive foraging. Our graphical approach explains this result by
222 demonstrating that the asymmetric coexistence cone found most frequently in nested networks
favors the extinction of specialist pollinators. To show this, we note that obtaining a supply point
224 in the orange region of Fig. 2c (where both specialist pollinator species go extinct) only requires
that the the supply level $\beta_3 p_3 / \phi_3$ of rewards 3 is greater than the supply of rewards 1. This
226 happens half of the time when the plant parameters are randomly chosen (as they were in the
previous simulations). But for the supply point to reach the blue and green region, where one
228 or both of the specialist pollinator species persist, the supply of rewards 3 must drop below the
ZNGI intersection. This is a much more stringent condition, and in practice it is only satisfied
230 when the specialist plant (here plant species 3) goes extinct (Fig. 2e).

232 To elucidate the conditions for plant extinction, we distinguish two drivers of species elimination:
competitive exclusion by other plant species for resources other than pollination, and failure

to receive sufficient pollination. Plant competition is modeled with a Lotka-Volterra type competition matrix and standard techniques from coexistence theory can be employed to study this aspect (see Appendix B). We focus on the second driver by assuming intraspecific competition much stronger than interspecific competition, which effectively gives each plant species its own niche. This leaves pollination – particularly visit quality (σ_{ij} , see Methods) – as the sole determinant of plant survival. Specialist plants receive the lowest quality of visits in nested networks, because they are only visited by generalist pollinators that carry diluted pollen from many other species. We find the criteria for plant survival by calculating the plant population size p_i as a function of the visit quality σ_{ij} for a perfectly specialist plant (visited by only one pollinator species). We obtained an exact analytic expression for this relationship (Eq. C5 of Appendix C), which is depicted in Fig. 2f. This relationship shows that each plant species remains near its maximum abundance ($1/w_i$) as long as the visit quality they receive is above a threshold σ_c , but it suddenly drops to zero when the visit quality drops below this threshold.

246 *Effects of adaptive foraging*

Adaptive foraging (Eq. 4) rotates the ZNGIs and impact vectors in the direction of the more plentiful floral rewards (see Methods). This section explains the consequences of this rotation for species coexistence and provides analytical understanding for the result found by previous simulations showing that adaptive foraging increases the species persistence of nested networks (Valdovinos et al. 2016).

Fig. 3 shows how adaptive foraging changes the result illustrated in Fig. 2a-c. The supply point lies just outside the coexistence cone, and the equilibrium state with fixed foraging preferences gives plant species 3 a higher equilibrium concentration of floral rewards. This means that the generalist pollinators will begin to focus their foraging efforts on plant species 3, resulting in a rotation of the ZNGI and impact vector to become more like those pollinators specialized on plant species 3 (i.e., a horizontal line and vertical arrow in this visualization). This rotation opens up the coexistence cone until it engulfs the supply point. The resource abundances then

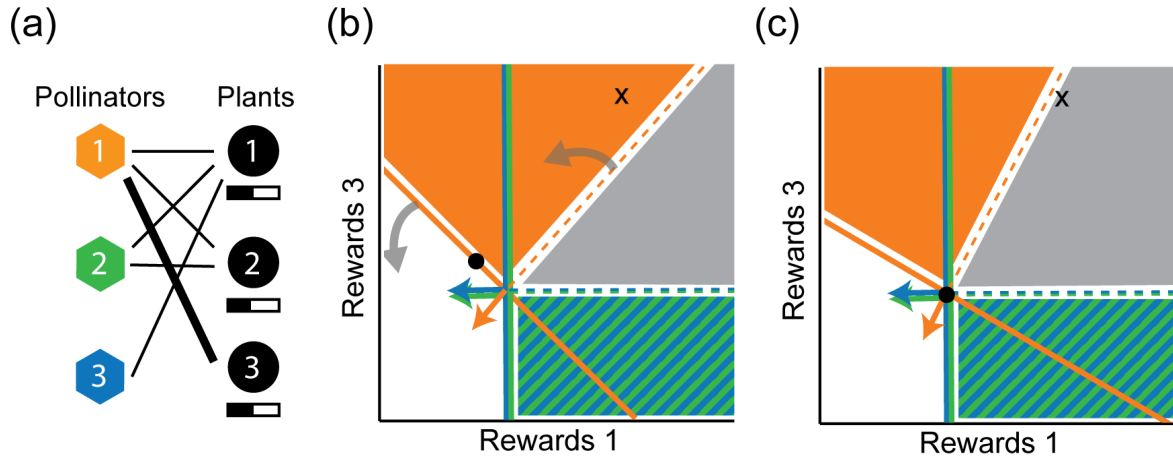


Figure 3: **Effects of adaptive foraging.** (a) Adding adaptive foraging to the nested network allows the generalist pollinators to focus their foraging effort on the plant species with more abundant floral rewards (thick line connecting pollinator 1 to plant 3). (b) Adaptive foraging causes the ZNGI of the generalist pollinator species and its impact vector to rotate counterclockwise (towards the most plentiful rewards 3). Black dot represents the equilibrium state of Fig. 2c, with more available rewards in plant species 3 than in species 1. (c) The rotation of the impact vector expands the coexistence cone making it to engulf the supply point, so that all three species coexist in the new equilibrium (black dot). This rotation also reduces the angle between the impact vector and the rewards 3 axis, increasing the quality of visits by the generalist pollinators to these plants, while decreasing their quality of visits to the other plant species.

relax to the coexistence point (R_1^*, R_2^*, R_3^*) , where all plants are equally good food sources, and

adaptation stops. This process allows the coexistence of all pollinator species.

Adaptive foraging increases coexistence among plant species in nested networks by causing pollinator species to focus their foraging efforts on more specialist plant species (Fig. 3a), increasing the visit quality they receive (see angle of the orange impact vector becoming more parallel to the rewards 3 axis in the sequence of Fig. 3b-c). This rotation in ZNGIs, in turn, decreases the visit quality that the generalist plants receive from the generalist pollinators (see angle of the orange impact vector becoming more perpendicular to the rewards 1 axis in the sequence of Fig. 3b-c). The generalist plant species will still persist despite this reduction in visit quality by

268 generalist pollinators, because they still receive perfect visit quality from specialist pollinators
269 that only visit them (e.g., pollinator species 3 in Fig. 3a) and which cannot shift their foraging
270 effort to other plant species. Overly-connected networks (i.e., with many more interactions than
271 the ones found in empirical networks) lack these perfect specialists and, therefore, the average
272 quality of visits received by generalist plant species drops below the threshold σ_c (Fig. 2c) and
273 they go extinct, as observed in previous simulations.

274 *Impact of pollinator invasions on native species*

275 This final section analyzes the consequences of pollinator invasions on species coexistence in
276 networks with adaptive foraging, and provides analytical understanding for the results found
277 numerically by Valdovinos et al. (2018). We assume that exotic species come from a different re-
278 gional pool, with consumption and mortality rates not following the strict relationship imposed
279 on the native species by Eq. 7. This results in the exotic's ZNGI not passing through the na-
280 tives' common ZNGI intersection (Fig. 4b,d), but instead intersecting different native ZNGI's at
281 different points. The resulting proliferation of possible coexistence points and cones impede the
282 analysis of high-dimensional systems using the method of projections employed above. There-
283 fore, we focus on a similar network than in previous sections but with only two (instead of three)
284 plant species.

285 Exotic pollinators will invade the network whenever the native coexistence point R_i^* falls on
286 the positive growth rate side of the exotic's ZNGI, regardless of the number of plant species the
287 exotic visits. This corresponds to the case of efficient foragers reported in previous simulations
288 (i.e., with higher foraging efficiency than natives), which were the only exotic pollinators invading
289 the networks studied by Valdovinos et al. (2018). The impact of the invader on native species
290 will depend on how the exotic's ZNGI alters the coexistence points which, in turn, depends on
291 the network structure.

292 A network structure with native pollinator species visiting only plant species visited by the
293 efficient invader (Fig. 4a), has three possible outcomes depending on the position of the sup-

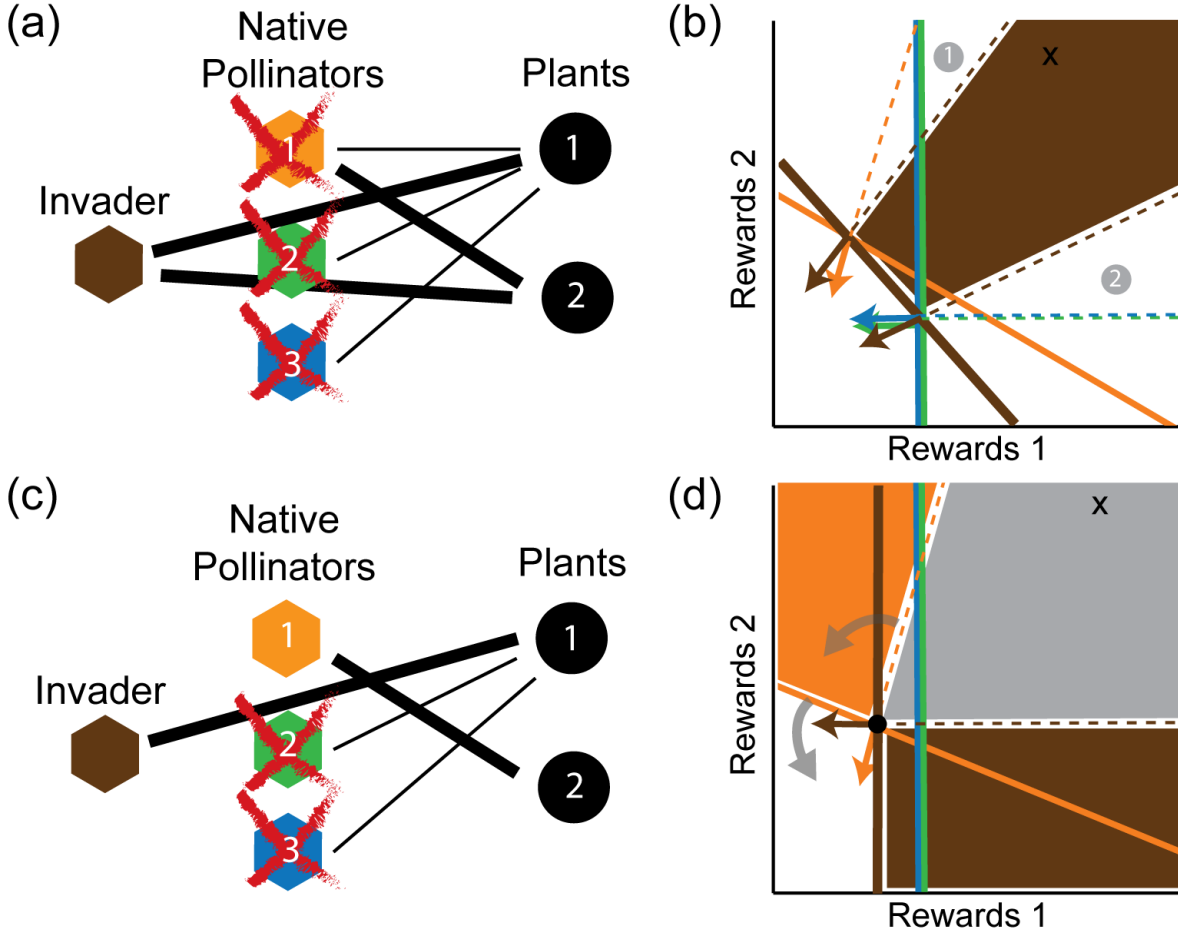


Figure 4: Pollinator invasions. (a) Brown polygon represents an exotic pollinator species with higher visit efficiency than natives, visiting the two plant species. (b) If plant species have similar abundances (as in previous simulations), the supply point falls in the gap between the two coexistence cones, and only the invader survives at equilibrium. (c) Invader does not interact with plant species 2. (d) The supply point now falls inside the coexistence cone 1 and the invader coexist with pollinator species 1. Adaptive foraging drives the native species to become a pure specialist on plant species 2 (which had more rewards). This results in plant species 2 receiving more and better visits, and in pollinator species 1 reducing its population size. The relative abundances can be estimated from the position of the supply point within the cone. For example, only a small contribution will be required from a pollinator species to achieve perfect cancellation of the supply if one of the other impact vectors points almost directly away from the supply point. The invader's impact vector points in slightly different directions at the two coexistence points. This results from the factor of R_i contained in the f_{ij} term of the impact vector as given in Table 2, which biases the vector in the direction of the more abundant reward. Plant extinctions do not occur under these conditions.

294 supply point: i) native specialists go extinct when the supply point falls in the invader-generalist
295 coexistence cone (cone 1 in Fig. 4b); ii) generalists go extinct when the supply point falls in the
296 invader-specialist coexistence cone (cone 2 in Fig. 4b); iii) all native pollinator species go extinct
297 when the supply point falls in the gap between the two coexistence cones (dark region in Fig. 4b).
298 This third outcome (illustrated in Fig. 4a) happens when all plant species have similar properties
299 (as assumed in previous simulations) which results in a supply point near the diagonal of the
300 rewards space.

A network structure where native pollinators visit plant species not visited by the invader
302 results in the coexistence between the invader and the natives that have access to those alternative
303 resources. For example, the pollinator species 1 coexists with the invader if the invader only
304 interacts with plant species 1. This results in plant species 2 having higher rewards than species
305 1 at the new coexistence point, which makes pollinator species 1 shift its foraging effort to plant
306 species 2 until it becomes a pure specialist (Fig. 4c). Conversely, all three pollinator species
307 coexist as specialists on plant species 1 if the invader only interacts with plant species 2.

308 This analysis suggests that native pollinators only visiting plants visited by the invader will
309 typically be driven extinct in larger networks, because the supply point will most likely fall in the
310 gap between the high-dimensional coexistence cones. But if a pollinator species interacts with
311 at least one plant species not visited by the invader, it will survive and transfer all its foraging
312 effort to these plants. This agrees with previous simulations.

Discussion

314 Previous studies on species coexistence in plant-pollinator systems mainly consisted of work de-
315 veloping conceptual (e.g., Palmer et al. 2003; Mitchell et al. 2009) and mathematical (e.g., Levin
316 and Anderson 1970; De Mazancourt and Schwartz 2010; Johnson and Bronstein 2019) frameworks
317 for analyzing conditions at which species can coexist, and reviews of empirical cases showing
318 competition among plant species for pollination services (e.g., Mitchell et al. 2009; Morales and

Traveset 2009) and among pollinator species for floral rewards (e.g., Palmer et al. 2003). The Contemporary Niche Theory allows a synthesis of all this information in one framework, and makes quantitative predictions about community dynamics including species coexistence. We expand this theory by incorporating plant-pollinator systems. Our contributions consist of considering short- and long-term dynamics of plant-pollinator interactions, depicting the requirement and impact niches of pollinators, and demonstrating the effect of adaptive foraging and network structure on those niches. We applied these advances to the understanding of pollinator invasions. We next explain each of these contributions and contextualize them with previous literature.

328 Explicit consideration of two timescales: Rewards and Plant Spaces

Explicit consideration of timescales has been recently highlighted as paramount for analyzing ecological systems, especially when evaluating management strategies (Callicott 2002; Hastings 2016) where the timeframe of action determines the ecological outcome. This is particularly the case of plant-pollinator systems whose dynamics can be distinctively divided into at least two timescales, the short-term dynamics occurring within a flowering season and the long-term dynamics occurring across flowering seasons. We developed our graphical approach for these short- and long-term dynamics by representing the pollinators' niches in Rewards and Plant Spaces, respectively. Rewards Space assumes approximately constant plant populations, analyzing the dynamics occurring during a flowering season where plants do not reproduce but produce floral rewards that are depleted by pollinators in a matter of hours or days. Plant Space represents the longer timescale at which the quality and quantity of pollinator visits impact plant populations represented on the axes.

The other work we know expanding Contemporary Niche Theory to mutualisms uses a more

classic consumer-resource space (Peay 2016), where niche axes represent resources in the soil used by plant species indistinctly of the timescale. That work shows how the plants' ZNGIs change when the mycorrhizal mutualism is added, but the axes are still resources in the soil, not

mutualists. In our work, by contrast, the axes are the abundances of the mutualistic partners

346 themselves (Plant Space) or the rewards produced by them (Rewards Space).

Depicting the pollinators' requirement and impact niches

348 Analysis of the requirement niches of species sharing resources has been long used to study
species coexistence (MacArthur 1970; Tilman 1982; Leibold 1995; Chase and Leibold 2003). Only
350 recently has such analysis been applied to mutualistic systems. Johnson and Bronstein (2019)
352 applied Tilman's Resource Ratio Theory to two pollinator species competing for the rewards
provided by one plant species, and when an abiotic resource is added. Our results expand
354 this work by extending to networks with larger numbers of plant and pollinator species, where
nestedness and adaptive foraging become relevant properties. However, we do not explicitly
356 consider resources or abiotic limitations other than floral rewards that species might require to
survive (e.g., nesting sites, water), which represents an important avenue for future work.

We study the pollinators' impact niche corresponding to the change induced on plant and
358 reward abundances. In Plant Space, the mutualism is directly visible in the impacts, which
represent the number of successful pollination events caused by each pollinator, and the impact
360 vectors point in the direction of larger plant population sizes. This space shows a main difference
between resource competition in classic consumer-resource and mutualistic systems. Consumers
362 in classic consumer-resource systems can only affect each other negatively through depleting
their shared resource, while consumers in mutualistic systems can also benefit each other through
364 benefiting their shared mutualistic partner. In Rewards Space, the impact of a pollinator species
is simply the rate at which it depletes the floral rewards, just as in a classic model of resource
366 competition. An important difference, however, is the representation of the visit quality of a
particular pollinator species to a particular plant species in terms of the angle between its impact
368 vector and the rewards axis corresponding to the plant species. The analysis of this representation
advances another subject that has captured the attention of ecologists for over a century, plant
370 competition for pollination (reviewed in Mitchell et al. 2009). This large body of research has

shown that plant species sharing the same pollinator species potentially compete not only for the
372 pollinators' quantity of visits but also for their quality of visits. Our approach provides means
for analyzing plant competition for quantity and quality of visits quantitatively and, therefore,
374 complements previous empirical and conceptual approaches.

Finally, the strict constraint on pollinator parameter values given by Eq. (7) highlights the in-
376 trinsic incompleteness of any model (including ours) that focuses exclusively on plant-pollinator
interactions, which are only a subset of the full ecosystem (Hale et al. 2020). Questions on how
378 many pollinator species can coexist or how to prevent competitive exclusion (Gause and Witt
1935; Levin 1970; McGehee and Armstrong 1977) present interesting avenues for further study in
380 models that consider the broader ecological and evolutionary context of plant-pollinator interac-
tions.

382 *Effects of network structure and adaptive foraging on species coexistence*

The network structure of plant-pollinator systems influences community dynamics and species
384 coexistence by determining who interacts with whom and which mutualistic partners are shared
between any two given species. We analyzed the effects of nestedness on species persistence in
386 these networks by depicting the dynamics occurring in systems where generalist and specialist
pollinators share the floral rewards of generalist plants, while specialist plants are visited only
388 by generalist pollinators. We provided analytical understanding to results found by previous
simulations by showing how nestedness with its increased niche overlap produces an asymmetric
390 coexistence cone that causes the extinction of specialist species.

We demonstrated that adaptive foraging rotates the pollinators' ZNGIs and impact vectors to-
392 wards the most abundant rewards, promoting pollinator coexistence in nested networks through
niche partitioning and plant coexistence through the increased visit quality to specialist plants.
394 We anticipate that our graphical representation of adaptive foraging can be applied to other types
of consumer-resource systems such as food webs, where the effects of adaptive foraging have
396 been extensively studied theoretically (reviewed in Valdovinos et al. 2010). For example, Kondoh

(2003) shows how adaptive foraging causes many species to coexist in complex food webs. Key
398 to this result is the “fluctuating short-term selection on trophic links”, which effectively reduces
the realized food-web connectance. That is, adaptive foraging allows the rare prey to recover by
400 making the consumers effectively specialize on the most abundant prey, which results in the rare
prey becoming more abundant and the abundant prey becoming more rare, causing the adaptive
402 consumers to switch their preferences again. This is similar to our result of generalist pollinators
becoming effectively specialized on specialist plants with initially higher reward abundance, but
404 is also different because our plant-pollinator model does not exhibit fluctuations in foraging pref-
erences. This difference is explained by the inherent timescales of rewards and prey dynamics,
406 where the rewards are produced and consumed at the same short timescale, while the production
of new prey are lagged behind the consumption by predators. We anticipate that our graphical
408 approach will deepen the conceptual unification of theory on mutualistic systems and theory on
food webs, by providing analytical understanding of species coexistence in consumer-resource
410 systems, and incorporating the effects of adaptive foraging and network structure, both critical
for the dynamics of those two types of consumer-resource systems.

412

Conclusion

Our graphical approach promotes the unification of niche and network theories by incorporating
414 network structure and adaptive foraging into the graphical representation of species’ niches.
This approach also deepens the synthesis of mutualistic and exploitative interactions within a
416 consumer-resource framework, by including both in the graphical representation of pollinators’
niches. This research may promote further development of ecological theory on mutualisms,
418 which is crucial for answering fundamental questions and informing conservation efforts.

Acknowledgments

⁴²⁰ We thank George Kling for his comments on earlier versions of this manuscript. This research was funded by US NSF (DEB-1834497) to FSV.

⁴²² Literature Cited

Allesina, S., and S. Tang. 2012. Stability criteria for complex ecosystems. *Nature* 483:205.

⁴²⁴ Bascompte, J., and P. Jordano. 2014. Mutualistic networks. Princeton University Press, Princeton, NJ.

⁴²⁶ Bascompte, J., P. Jordano, and J. Olesen. 2006. Asymmetric coevolutionary networks facilitate biodiversity maintenance. *Science* 312:431.

⁴²⁸ Bastolla, U., M. Fortuna, A. Pascual-García, A. Ferrera, B. Luque, and J. Bascompte. 2009. The architecture of mutualistic networks minimizes competition and increases biodiversity. *Nature* 458:1018.

⁴³⁰ Boucher, D., S. James, and K. Keeler. 1982. The ecology of mutualism. *Annual Review of Ecology and Systematics* 13:315.

⁴³² Bronstein, J. 2015. The study of mutualism. *In* J. Bronstein, ed., Mutualism. Oxford University Press, Oxford.

Brown, B. E. 1997. Coral bleaching: causes and consequences. *Coral Reefs* 16:S129.

⁴³⁴ Callicott, J. B. 2002. Choosing appropriate temporal and spatial scales for ecological restoration. *Journal of Biosciences* 27:409–420.

⁴³⁶ Chase, J. M., and M. A. Leibold. 2003. Ecological niches: linking classical and contemporary approaches. University of Chicago Press, Chicago, IL.

440 Chesson, P. 2000. Mechanisms of maintenance of species diversity. *Annual review of Ecology and Systematics* 31:343.

442 De Mazancourt, C., and M. W. Schwartz. 2010. A resource ratio theory of cooperation. *Ecology letters* 13:349–359.

444 Gause, G. F., and A. A. Witt. 1935. Behavior of mixed populations and the problem of natural selection. *The American Naturalist* 69:596.

446 Goulson, D., E. Nicholls, C. Botías, and E. Rotheray. 2015. Bee declines driven by combined stress from parasites, pesticides, and lack of flowers. *Science* 347:1255957.

448 Hale, K. R., F. S. Valdovinos, and N. D. Martinez. 2020. Mutualism increases diversity, stability, and function of multiplex networks that integrate pollinators into food webs. *Nature Communications* 11:1–14.

450 Hastings, A. 2016. Timescales and the management of ecological systems. *Proceedings of the National Academy of Sciences* 113:14568–14573.

452 Hershkowitz, D., and N. Keller. 2003. Positivity of principal minors, sign symmetry and stability. *Linear algebra and its applications* 364:105–124.

454 Holland, J., and D. DeAngelis. 2010. A consumer-resource approach to the density-dependent population dynamics of mutualism. *Ecology* 91:1286.

456 Holland, J., J. Ness, A. Boyle, and J. Bronstein. 2005. Mutualisms as consumer-resource interactions. *Ecology of predator–prey interactions* page 17.

458 Holling, C. S. 1959. Some characteristics of simple types of predation and parasitism. *The Canadian Entomologist* 91:385.

460 Horton, T., and T. Bruns. 2001. The molecular revolution in ectomycorrhizal ecology: peeking into the blackbox. *Mol. Ecol.* 10:1855.

Johnson, C., and J. Bronstein. 2019. Coexistence and competitive exclusion in mutualism. *Ecology* 100:e02708.

Koffel, T., T. Daufresne, F. Massol, and C. A. Klausmeier. 2016. Geometrical envelopes: Extending graphical contemporary niche theory to communities and eco-evolutionary dynamics. *Journal of Theoretical Biology* 407:271.

Kondoh, M. 2003. Foraging adaptation and the relationship between food-web complexity and stability. *Science* 299:1388–1391.

Kostitzin, V. 1934. *Symbiose, Parasitisme et Evolution (Etude Mathematique)*. Hermann et Cie, Paris.

Leibold, M. A. 1995. The niche concept revisited: mechanistic models and community context. *Ecology* 76:1371–1382.

Levin, D. A., and W. W. Anderson. 1970. Competition for pollinators between simultaneously flowering species. *The American Naturalist* 104:455–467.

Levin, S. A. 1970. Community equilibria and stability, and an extension of the competitive exclusion principle. *The American Naturalist* 104:413.

MacArthur, R. 1969. Species packing, and what competition minimizes. *Proceedings of the National Academy of Sciences* 64:1369.

———. 1970. Species packing and competitive equilibrium for many species. *Theoretical population biology* 1:1–11.

McGehee, R., and R. A. Armstrong. 1977. Some Mathematical Problems Concerning the Ecological Principle of Competitive Exclusion. *Journal of Differential Equations* 23:30.

Mitchell, R. J., R. J. Flanagan, B. J. Brown, N. M. Waser, and J. D. Karron. 2009. New frontiers in competition for pollination. *Annals of Botany* 103:1403–1413.

486 Morales, C. L., and A. Traveset. 2009. A meta-analysis of impacts of alien vs. native plants on
488 pollinator visitation and reproductive success of co-flowering native plants. *Ecology Letters*
12:716–728.

490 Okuyama, T., and J. Holland. 2008. Network structural properties mediate the stability of mutu-
492 alistic communities. *Ecol. Lett.* 11:208.

Ollerton, J. 2017. Pollinator diversity: distribution, ecological function, and conservation. *Annu.*
492 *Rev. Ecol. Evol. Syst.* 48:353.

494 Ollerton, J., R. Winfree, and S. Tarrant. 2011. How many flowering plants are pollinated by
animals? *Oikos* 120:321.

496 Pacciani-Mori, L., A. Giometto, S. Suweis, and A. Maritan. 2020. Dynamic metabolic adaptation
can promote species coexistence in competitive communities. *PLOS Computational Biology*
16:e1007896.

498 Palmer, T. M., M. L. Stanton, and T. P. Young. 2003. Competition and coexistence: exploring
mechanisms that restrict and maintain diversity within mutualist guilds. *The American Natu-
500 ralist* 162:S63–S79.

502 Peay, K. 2016. The mutualistic niche: Mycorrhizal symbiosis and community dynamics. *Annu.*
502 *Rev. Ecol. Evol. Syst.* 47:143.

504 Potts, S., V. Imperatriz-Fonseca, H. Ngo, M. Aizen, J. Biesmeijer, and T. Breeze. 2016. Safeguarding
pollinators and their values to human well-being. *Nature* 540:220.

Rowan, R. 2004. Coral bleaching: thermal adaptation in reef coral symbionts. *Nature* 430:742.

506 Tilman, D. 1982. *Resource competition and community structure*, vol. 17. Princeton University
Press.

508 Valdovinos, F. S. 2019. Mutualistic networks: moving closer to a predictive theory. *Ecology*
Letters 22:1517.

510 Valdovinos, F. S., E. L. Berlow, P. M. De Espanés, R. Ramos-Jiliberto, D. P. Vázquez, and N. D. Martinez. 2018. Species traits and network structure predict the success and impacts of pollinator invasions. *Nature Communications* 9:2153.

512

514 Valdovinos, F. S., B. J. Brosi, H. M. Briggs, P. Moisset de Espanés, R. Ramos-Jiliberto, and N. D. Martinez. 2016. Niche partitioning due to adaptive foraging reverses effects of nestedness and connectance on pollination network stability. *Ecology Letters* 19:1277.

516 Valdovinos, F. S., P. Moisset de Espanés, J. D. Flores, and R. Ramos-Jiliberto. 2013. Adaptive foraging allows the maintenance of biodiversity of pollination networks. *Oikos* 122:907.

518 Valdovinos, F. S., R. Ramos-Jiliberto, L. Garay-Varváez, P. Urbani, and J. A. Dunne. 2010. Consequences of adaptive behaviour for the structure and dynamics of food webs. *Ecology Letters* 13:1546–1599.

520

522 van der Heijden, M., R. Bardgett, and N. van Straalen. 2008. The unseen majority: soil microbes as drivers of plant diversity and productivity in terrestrial ecosystems. *Ecology Letters* 11:296.

524 Vandermeer, and Boucher. 1978. Varieties of mutualistic interaction in population models. *J. Theor. Biol.* 74:549.

526 Wang, B., and T. Smith. 2002. Closing the seed dispersal loop. *Trends in Ecology & Evolution* 17:379.

528 Wolin, C., and L. Lawlor. 1984. Models of facultative mutualism: Density effects. *The American Naturalist* 124:843.

530 Yodzis, P., and S. Innes. 1992. Body size and consumer-resource dynamics. *The American Naturalist* 139:1151.

Appendix A: Analysis of adaptive foraging equation

532 In this appendix, we show that the adaptive foraging dynamics given in Eq. (4) of the main text
cause the ZNGI of a pollinator species j to rotate about a point in rewards space, whose coordinates
534 are given by the minimum reward abundance R_{ij}^* required for the pollinator to survive under a pure specialist strategy focused on plant species i .

First of all, setting $da_j/dt = 0$ in Eq. (2) of the main text, with $\alpha_{ij} = 1$ and $\alpha_{kj} = 0$ for all $k \neq i$, we obtain the equilibrium condition under the pure specialist strategy:

$$0 = c_{ij}\tau_{ij}b_{ij}a_jR_i - \mu_j^A a_j. \quad (\text{A1})$$

Solving for the reward abundance, we obtain:

$$R_{ij}^* = \frac{\mu_j^A}{c_{ij}\tau_{ij}b_{ij}}. \quad (\text{A2})$$

536 This is the same as Eq. (7) of the main text, but we have added an index j to indicate that this point can in general be different for each pollinator species, depending on the choice of
538 parameters.

Next, we confirm that the adaptive foraging dynamics of Eq. (4) preserve the constraint $\sum_{i \in P_j} \alpha_{ij} = 1$ imposed in the initial conditions, by computing

$$\frac{d}{dt} \sum_{i \in P_j} \alpha_{ij} = G_j \sum_{i \in P_j} \alpha_{ij} \left(c_{ij}\tau_{ij}b_{ij}R_i - \sum_{k \in P_j} \alpha_{kj}c_{kj}\tau_{kj}b_{kj}R_k \right) \quad (\text{A3})$$

$$= G_j \left(1 - \sum_{i \in P_j} \alpha_{ij} \right) \sum_{k \in P_j} \alpha_{kj}c_{kj}\tau_{kj}b_{kj}R_k. \quad (\text{A4})$$

Thus if $\sum_{i \in P_j} \alpha_{ij} = 1$ at any point in time, the derivative vanishes, and it remains equal to this
540 value for all times.

Finally, we show that this constraint on the sum of α_{ij} guarantees that the point R_{ij}^* defined

above always lies on the ZNGI, i.e., that da_j/dt always vanishes there:

$$\frac{da_j}{dt} = \sum_{i \in P_j} c_{ij} \alpha_{ij} \tau_{ij} b_{ij} a_j R_{ij}^* - \mu_j^A a_j \quad (\text{A5})$$

$$= \sum_{i \in P_j} \alpha_{ij} \mu_j^A a_j - \mu_j^A a_j = 0. \quad (\text{A6})$$

Appendix B: Conditions for coexistence among plant species

542 Unlike the population growth rate of pollinators that entirely depends on rewards abundances,
 the population growth rate of plants in the Valdovinos et al. model considers other factors (e.g.,
 544 space or nutrient limitation) that are captured by a generic Lotka-Volterra type function of plant
 competition composed of intra- (or self-limitation) and inter-specific competition coefficients (w_i
 546 and u_l , respectively) that affect plant recruitment rate (γ_i in Eq. D3) and are independent of the
 mutualistic interaction with pollinators. The standard conditions for stable coexistence in Lotka-
 548 Volterra models therefore represent a necessary condition for plant coexistence. Whether a plant
 species actually persists at equilibrium also depends on whether it receives sufficient pollination
 550 services, which will be discussed in Appendix C below.

To simplify our analysis, in the main text we focus on the case of low inter-specific competition
 552 (i.e., $u_l \ll w_i$), which is also the regime where all the relevant numerical simulations were
 performed (Valdovinos et al. 2013, 2016, 2018), so we can safely approximate $p_i^* \approx 1/w_i$ under
 554 conditions of adequate pollination.

To go beyond this regime, and obtain necessary coexistence conditions with non-negligible
 interspecific competition, we must examine the stability of the fixed points of the plant dynam-
 ics given by Eq. (1). To keep the problem tractable, we will treat α_{ij} as fixed parameters, and
 assume that a_j quickly relax to the equilibrium value $a_j^*(p_k)$ corresponding to the current plant
 abundances. Under these assumptions, the stability of the plant equilibrium depends on the

eigenvalues of the Jacobian matrix

$$J_{ik} = \frac{\partial}{\partial p_k} \frac{dp_i}{dt} = \frac{\partial \gamma_i}{\partial p_k} \sum_{j \in A_i} e_{ij} \sigma_{ij} V_{ij} + \gamma_i \frac{\partial}{\partial p_k} \sum_{j \in A_i} e_{ij} \sigma_{ij} V_{ij} - \mu_i^P \delta_{ik}, \quad (\text{B1})$$

evaluated at the equilibrium point p_i^* . If all eigenvalues have negative real parts, then the equilibrium is stable.

To further streamline the calculation, we will assume that $w_i = w$ for all i and $u_l = u$ for all l . This allows us to state the results in terms of the relative strength of interspecific (u) versus intraspecific (w) competition. Evaluating the derivatives, we then find:

$$J_{ik} = - \left(g_i \sum_{j \in A_i} e_{ij} \sigma_{ij} V_{ij} \right) [(w - u) \delta_{ik} + u] + \gamma_i \sum_{j \in A_i} e_{ij} \sigma_{ij} \alpha_{ij} \tau_{ij} p_i^* \frac{\partial a_j^*}{\partial p_k} + \left(\gamma_i \sum_{j \in A_i} e_{ij} \sigma_{ij} \alpha_{ij} \tau_{ij} a_j^* - \mu_i^P \right) \delta_{ik}. \quad (\text{B2})$$

The final term in parentheses is equal to $d \log p_i / dt$ for $p_i > 0$, and so it must vanish whenever all the plants coexist. To determine the sign of the eigenvalues for the remaining portion, it is convenient to define the diagonal matrix \mathbf{D} with components

$$D_{ik} = \delta_{ik} g_i \sum_{j \in A_i} e_{ij} \sigma_{ij} V_{ij} \quad (\text{B3})$$

and a matrix \mathbf{A} with components

$$A_{ik} = \frac{\gamma_i \sum_{j \in A_i} e_{ij} \sigma_{ij} \alpha_{ij} \tau_{ij} p_i^* \frac{\partial a_j^*}{\partial p_k}}{g_i \sum_{j \in A_i} e_{ij} \sigma_{ij} V_{ij}}. \quad (\text{B4})$$

We can now write the Jacobian \mathbf{J} in matrix notation as

$$\mathbf{J} = -\mathbf{D}[(w - u)\mathbf{I} + \mathbf{U} - \mathbf{A}] \quad (\text{B5})$$

where \mathbf{I} is the identity matrix and \mathbf{U} is a matrix with elements $U_{ij} = u$.

In the low mortality limit $\mu_i^P \rightarrow 0$, the steady state occurs at $\gamma_i \rightarrow 0$, and so $\mathbf{A} \rightarrow 0$. In this case, the eigenvalues of $[(w - u)\mathbf{I} + \mathbf{U}]$ can be evaluated exactly, with one eigenvalue equal to

$$\lambda^+ = w + (P - 1)u \quad (\text{B6})$$

and the rest equal to

$$\lambda^- = w - u. \quad (\text{B7})$$

558 For any symmetric matrix \mathbf{M} with all negative eigenvalues (a so-called “stable” matrix), the product \mathbf{DM} with any diagonal matrix \mathbf{D} with all positive entries also has all negative eigenvalues.

560 This property of maintaining stability under multiplication by a positive diagonal matrix \mathbf{D} is known as “D-stability,” and it has been proven that all sign-symmetric stable matrices are also

562 D-stable (Hershkowitz and Keller 2003). Applying this to the case at hand, we see that the eigenvalues of \mathbf{J} are all negative if and only if $\lambda^- > 0$. Thus we recover for arbitrary numbers of species

564 the classic result of modern coexistence theory for two species: stable coexistence requires that intra-specific competition (w) is stronger than inter-specific competition (u) (Chesson 2000).

To determine the impact of nonzero \mathbf{A} , we focus on the case where all pollinators are pure specialists, with identical parameters. Then \mathbf{A} is proportional to the identity matrix:

$$\mathbf{A} = \frac{1 - [(P-1)u + w]p^*}{a^*} \frac{\partial a^*}{\partial p} \mathbf{I} \quad (\text{B8})$$

where $p_i^* = p^*$ and $a_j^* = a^*$ for all i and j , since all the parameters are the same. Since the pollinators feed on the rewards produced by the plants, $\partial a^* / \partial p$ is always positive. The smallest eigenvalue of $[(w - u)\mathbf{I} + \mathbf{U} - \mathbf{A}]$ becomes

$$\lambda^- = \tilde{w} - u \quad (\text{B9})$$

where the effective intra-specific competition coefficient \tilde{w} is

$$\tilde{w} = w - \frac{1 - [(P-1)u + w]p^*}{a^*} \frac{\partial a^*}{\partial p} \quad (\text{B10})$$

566 which is always less than w . This means that the low-mortality criterion $w > u$ remains a necessary condition for coexistence. We conjecture that this remains true for arbitrary pollinator

568 parameters and connectivity, because it there is no obvious reason why competition between different species of pollinators should selectively provide additional intra-specific feedback for

570 the plants.

Appendix C: Minimum visit quality for specialist plants

We consider the equilibrium condition for a specialist plant of species i , which is visited by just one pollinator species j , obtained from Eq. (1) by substituting in for γ_i and V_{ij} using the linear model described in the first section of the Methods in the main text. We set $u_l = 0$, as discussed in the main text and in Appendix B, in order to obtain the minimal visit quality required for survival, under ideal conditions with no direct competition from other plant species. We find:

$$0 = \frac{dp_i}{dt} = g_i(1 - w_i p_i) e_{ij} \sigma_{ij} \tau_{ij} \alpha_{ij} a_j - \mu_i^p. \quad (\text{C1})$$

The pollinator population density a_j can be found by solving the equilibrium condition for the rewards, obtained from Eq. (3):

$$0 = \frac{dR_i}{dt} = \beta_i p_i - \phi_i R_i - b_{ij} \tau_{ij} \alpha_{ij} a_j R_i. \quad (\text{C2})$$

To solve this, we recall that in the equilibrium state of interest, where the adaptive foraging is also at equilibrium, the reward abundances are equal to R_i^* as defined in Eq. (7) of the main text.

Thus we arrive at:

$$a_j = \frac{\beta_i p_i - \phi_i R_i^*}{b_{ij} \tau_{ij} \alpha_{ij} R_i^*}. \quad (\text{C3})$$

Substituting into Eq. (C1), we have:

$$0 = g_i(1 - w_i p_i) e_{ij} \sigma_{ij} \frac{\beta_i p_i - \phi_i R_i^*}{b_{ij} R_i^*} - \mu_i^p. \quad (\text{C4})$$

This is a quadratic equation in p_i , which can be solved to obtain:

$$p_i = \frac{1}{w_i} \left[1 - \frac{1}{2} (1 - d_i) \left(1 - \sqrt{1 - \frac{4}{s_{ij} \sigma_{ij} (1 - d_i)}} \right) \right] \quad (\text{C5})$$

where

$$d_i = \frac{\phi_i R_i^* w_i}{\beta_i} \quad (\text{C6})$$

is the fraction of floral rewards that are lost to dilution when the plant population is at its carrying capacity $1/w_i$, and

$$s_{ij} = \frac{g_i e_{ij} \beta_i (1 - d_i)}{w_i \mu_i^P b_{ij} R_i^*} \quad (C7)$$

is the number of seedlings produced per plant lifetime under optimal conditions, where there are no other plant species nearby to contaminate the pollen, and the field is kept clear of all competing plants. Specifically, $g_i e_{ij}$ is the number of individual seedlings produced per pollinator visit, $(1 - d_i) \beta_i / (\mu_i^P w_i)$ is the harvested rewards mass per unit area over the plant's lifetime (i.e., over the average lifetime of an individual plant in the corresponding stochastic version of this model), and $b_{ij} R_i^*$ is the rewards mass density harvested per visit.

Appendix D: Saturating functional responses

In the version of the model presented in the main text, which was employed in all the previous simulations, the pollinator growth rates are linear functions of rewards abundances. In reality, both the quantity of rewards extracted per visit f_{ij} and the visit frequency V_{ij} are likely to saturate at high rewards levels. All the qualitative results obtained in the main text apply to these more realistic models as well. In this Appendix, we provide mathematical expressions for these two types of saturation, along with the expressions corresponding to Eq. (7) of the main text that specify the point R_i^* in rewards space where adaptive foraging reaches a nontrivial steady state.

The original publication presenting the model (Valdovinos et al. 2013) contained a discussion of saturating rewards extraction, with each pollinator capable of obtaining a finite quantity b_{ij}^{\max} of rewards per visit, following Holling's Type II growth kinetics (Holling 1959):

$$f_{ij} = b_{ij}^{\max} \frac{R_i}{\kappa_{ij} p_i + R_i}. \quad (D1)$$

Setting $da_j/dt = 0$ and $\alpha_{kj} = \delta_{ik}$ in Eq. 2 and substituting in with this formula for f_{ij} , we find that the equilibrium rewards level R_{ij}^* for the specialist strategy satisfies:

$$c_{ij} \tau_{ij} b_{ij}^{\max} = \mu_j^A \frac{\kappa_{ij} p_i + R_{ij}^*}{p_i R_{ij}^*} \quad (D2)$$

586 This equation reveals a set of two sufficient conditions to give all pollinator species j the same
 R_{ij}^* (as required for adaptive foraging to admit of a steady state with all these species sharing
588 rewards from species i): (i) the mass-specific rewards uptake rates $c_{ij}\tau_{ij}b_{ij}^{\max}$ for different j must
scale linearly with the mortality rates μ_j^A , and (ii) κ_{ij} must be the same for all j .

In addition to the finite capacity of a pollinator to extract rewards on each visit, it is reasonable to assume that there is a maximum number of visits that an animal can make per unit time. Using the same Type II kinetics, we obtain the following expression for the total visitation rate of pollinator species j on plant species i :

$$V_{ij} = a_j \frac{\tau_{ij}\alpha_{ij}p_i}{1 + \sum_k \tau_{kj}\alpha_{kj}h_{kj}p_k + \sum_k \omega_{jk}a_k}. \quad (\text{D3})$$

Here h_{kj} is the handling time for pollinator species j foraging on plant species k , and ω_{jk} quantifies the magnitude of direct interference between pollinators. Direct interference significantly complicates the geometric interpretation, so we will set $\omega_{jk} = 0$ here. If the saturation of visit frequency is the only relevant nonlinearity, and the rewards uptake per visit is still linear in R_i , then the ZNGIs remain linear. When both kinds of saturation are present, the specialist equilibrium point R_{ij}^* is defined by:

$$c_{ij}\tau_{ij}b_{ij}^{\max} = \mu_j^A \frac{(\kappa_{ij}p_i + R_{ij}^*)(1 + \sum_k \tau_{kj}\alpha_{kj}h_{kj}p_k)}{p_i R_{ij}^*}. \quad (\text{D4})$$

590 Giving all species the same set of R_{ij}^* requires two more assumptions beyond what was required
for saturating rewards extraction alone: (i) the handling time h_{kj} must be inversely proportional
592 to the visitation efficiency τ_{kj} for all pollinator species j visiting a given plant species k , and (ii)
all the plant population densities (for non-extinct plants) must be the same. Both of these are
594 trivially satisfied under conditions similar to the simulations discussed in the main text, where
the only differences between species come from the topology of the interaction network, and all
596 other parameters are species-independent.

Fig. S1 shows that the ZNGIs are no longer linear under saturating rewards extraction, but
598 that the graphical arguments from the main text still hold. The key point is that when all parameters are species-independent (except for interaction network topology) the initial impact vectors

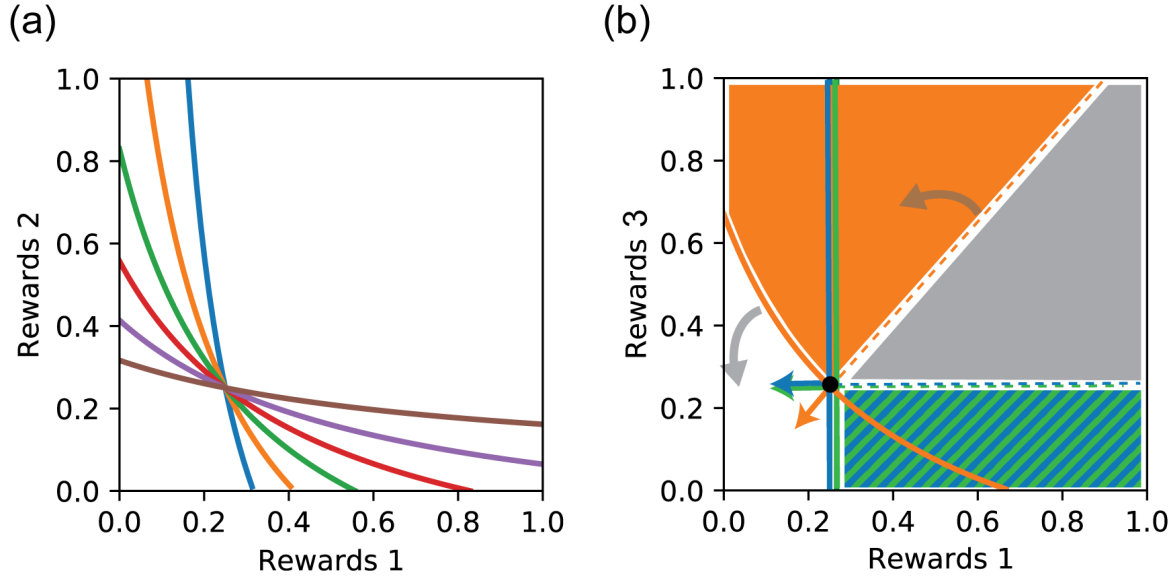


Figure S1: **Saturating growth laws.** (a) Scaling the maximum mass-specific rewards uptake rate $c_{ij}\tau_{ij}b_{ij}^{\max}$ with the pollinator mortality rate μ_j^A ensures that all species have the same minimum viable rewards level R_{ij}^* under a specialist strategy on each plant species i . As in the linear model, this implies that all ZNGIs cross at this point, and rotate about it during adaptive foraging. (b) ZNGIs, impact vectors, supply vector and coexistence cone for the nested network of Fig. 2, with saturating rewards uptake following Eq. (D1). Gray arrows indicate the direction of rotation of the ZNGI and coexistence cone boundary under adaptive foraging.

600 are required by symmetry to be perpendicular to the ZNGIs, and adaptive foraging tends to
 601 rotate them away from the rewards axes corresponding to generalist plants, just as in the linear
 602 model. Since these are the two essential features necessary for recovering the simulation results,
 we expect that the same phenomena will be observed even in the presence of saturation.

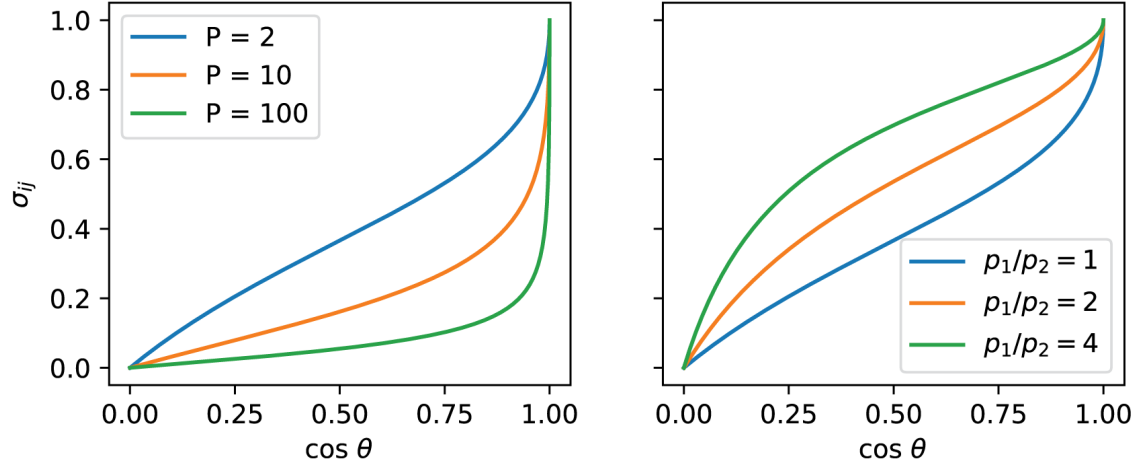


Figure S2: **Relation between angle and quality.** Left: Visit quality $\sigma_{ij} = \alpha_{ij}\tau_{ij}p_i / \sum_{k \in P_j} \alpha_{kj}\tau_{kj}p_k$ versus cosine of the angle θ between the impact vector of pollinator species j and (negative) rewards axis i ($\cos \theta = \alpha_{ij}\tau_{ij}b_{ij} / \sum_{k \in P_j} (\alpha_{kj}\tau_{kj}b_{kj})^2$). All plants are assumed to have identical abundances p_i , all foraging efficiencies τ_{ij} and per-visit rewards extraction b_{ij} are equal, and the foraging effort not expended on plant i is equally distributed over all other plant species. Each line represents a different value of the total number of plant species P . Right: Same as previous panel, but for $P = 2$, and different values of the ratio p_1/p_2 of the two plant abundances. Note that $\sigma_{ij} = 0$ always corresponds to $\cos \theta = 0$, and $\sigma_{ij} = 1$ always corresponds to $\cos \theta = 1$, and that between these two extremes the relationship is always monotonic.

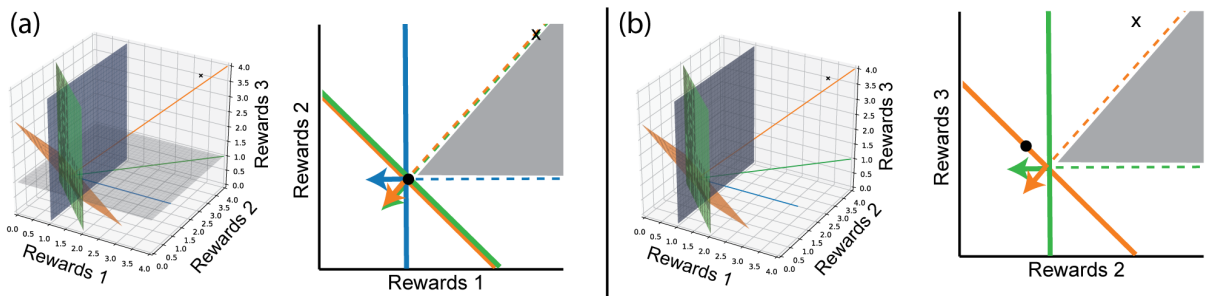


Figure S3: **Additional projections.** Projections of the three-plant, three-pollinator system of Fig. 2 onto the other two planes: (a) Rewards 1/Rewards 2 (b) Rewards 2/Rewards 3. Note that the blue species is not visible in the second projection, because the ZNGI is parallel to the projection plane, and the impact vector is perpendicular to the plane.

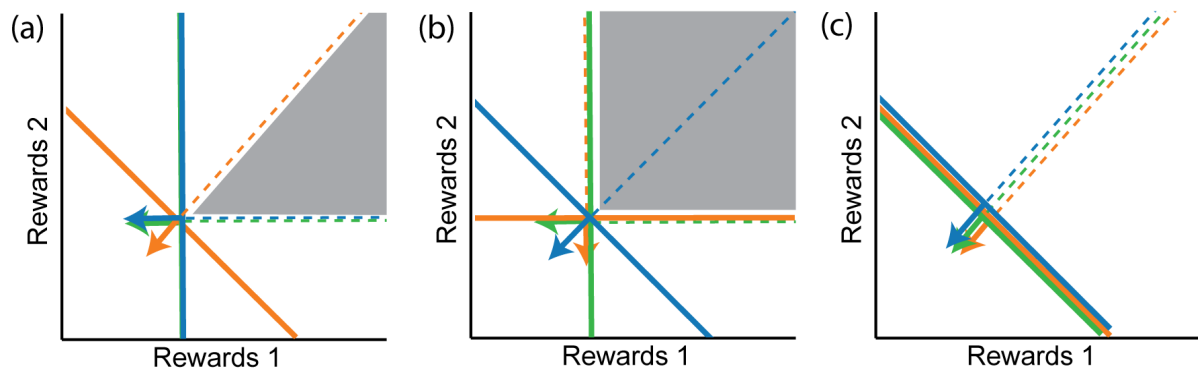


Figure S4: **Complete set of possible projections without AF.** There are only three distinct two-dimensional projections of the coexistence cone that are possible in the absence of adaptive foraging. The shape of the projected cone depends only on the existence of pollinators that service one of the two plants in the projection but not the other. (a) One plant has a specialist pollinator. (b) Both plants have specialist pollinators. (c) Neither plant has a specialist pollinator.